

# ADAPTIVE FLIGHT CONTROL USING SMOOTH BOUNDED CANDIDATE FUNCTIONS

J. Seifert, Bauhaus Luftfahrt e.V., Germany  
F. Holzapfel, Institute for Flight Dynamics, Germany  
Technische Universität München, Boltzmannstr. 15, 85748 Garching

## Abstract

The development of a digital flight control system for new aircraft is usually based on a representative numerical flight simulation model. The quality of such a simulation is dependent on the quality of the aerodynamic model and the design of the flight control system. The paper proposes a strategy to relax the efforts required for model and controller parameter determination.

The motivation for this method is to deal with uncertainties in the aerodynamic model and to improve the control capability of flight control systems by adaptation to the true system behavior. New approaches have been investigated in order to improve either the aerodynamic model [2] or the flight control system by online adaption [1]. The application of an adaptive element in a flight management system provides new prospects for the automatic guidance of unmanned air vehicles, even in the case of system degradation. For example, a Modular Neural Network (MNN) could be such an adaptive element. In general, Neural Networks have the capability to approximate any continuous function [4]. Furthermore a well structured MNN based on a-priori knowledge enhances the possibility of monitoring the characteristic system parameters [3].

A MNN derived feed-forward controller with a proportional error feedback loop is used in this example. It is demonstrated in principle, how a conventional control structure can be extended to a MNN structure. Furthermore a new definition of a network-error-signal and a new method for error propagation and finally system learning is shown. The capability of this method is demonstrated using numerical flight simulation.

## 1. INTRODUCTION

The motivation for an adaptive flight control using smooth bounded candidate functions evolved from recent developments in the area of Unmanned Air Systems (UAS). The design space for future air systems has been expanded by technologies such as morphing structures leading to unconventional designs of the airframe. In particular, the transition between two configuration setups (e.g. vertical take-off and cruise flight) during operation is a crucial point for flight control.

In the area of adaptive flight control many successful studies were performed, demonstrating the capability of online adaptation during system operation [6]. Conventional flight control systems have been augmented with an adaptive element, to handle uncertainties in the reference model or a failure in the system [1]. This evolution raises the question, if a future adaptive flight control system could be designed on the basis of controller gains, which are adapted during operation and are smoothly bounded to a predefined limit?

A successful application of a MNN on aerodynamic parameter identification using the so called input-weights was demonstrated in [2]. Within this contribution here the

results of a conceptual study will be shown, in order to reveal, if such a method can be transferred to an application in flight control.

Artificial neural networks use smooth bounded candidate functions to approximate arbitrary nonlinear maps. The sigmoid function is often used as activation function.

For the neural network learning process often an algorithm called Backpropagation is used. This is an error-based gradient descent method adjusting the weights of the links between multiple layers of neurons. With a modular structure of the neural network it is possible to assign an area of the network model to a certain physical effect.

If the need for low-cost systems in the field of UAS will increase, adaptive flight control will be a solution to reduce the costs of system development. One possible solution is presented here, a combination of Neural Network technologies combined with state-of-the-art Adaptive Control techniques.

## 2. ADAPTIVE CONTROL

An adaptive controller differs from an ordinary controller in that either controller gains or model parameters are variable, and there is an algorithm for adapting these gains

online, based on signals in the system. One approach for constructing an adaptive controller is investigated here, using the model-reference adaptive control method (MRAC).

## 2.1. Model-Reference Adaptive Control

A model-reference adaptive control system according to Slotine [5] for a roll-command-system is given in FIGURE 1. If the parameters of the aircraft model are not known, the adaptation mechanism will adjust the controller parameters so that perfect tracking of the reference model is asymptotically achieved.

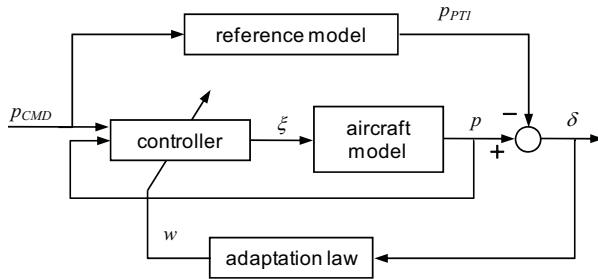


FIGURE 1: Model-reference adaptive control system for the roll-axis of the aircraft model

## 2.2. Aircraft Model

The simulation used for this investigation consists of a six degree of freedom nonlinear aircraft model. The aerodynamic model is composed out of the major derivatives and the application rules offer the possibility to adjust the parameters for test purposes. There are simple sensor and actuator models which do not represent the dynamic response of the original parts.

The flight control is realized as rate-command-system. One part of the controller, the roll axis, was exchanged by adaptive control. The yaw and pitch axis were not modified.

## 2.3. Reference Model

A reference model is used to specify the ideal response of the adaptive control system to the external command. It should provide the ideal aircraft response which the adaptation mechanism should seek in adjusting the controller gains  $k_v$  and  $k_p$ . There are constraints for the choice of the reference model, as it has to satisfy two requirements. On the one hand, it should reflect the performance specification in the control tasks, such as rise time, settling time, overshoot or frequency domain characteristics. On the other hand, this ideal behavior should be achievable for the adaptive control system.

Here is a simplified representation of the aircraft dynamics selected. A first-order-system with a  $PT_1$  response was considered as a representative physical reference model:

$$(1) \quad T \cdot \dot{p}_{PT1} + p_{PT1} = K \cdot p_{CMD}$$

For a commanded roll rate  $p_{CMD} = 20^\circ/s$  a target function  $p_{PT1}$  is calculated from equation (1) and shown in FIGURE 2:

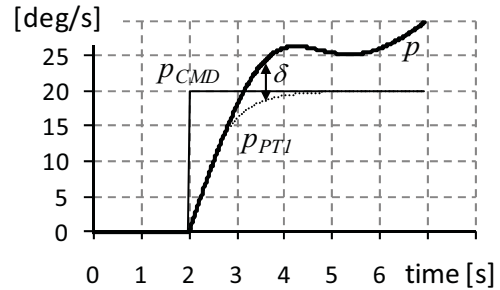


FIGURE 2: response of the reference model and the aircraft model after a step input command

## 2.4. Controller

A controller with feedforward gain and a proportional error feedback was designed with least complexity on the basis of Modular Neural Network technique [3]. Unlike conventional neural networks (e.g. MLP) that yield only black-box models, the structure and parameters of this kind of structured network are interpretable and can be monitored during the training phase. This capability is realized by using 'input-weights' for the controller input  $p$  and  $p_{CMD}$ . Here, the simple structure would not require the use of such networks – linear parameters would be sufficient. However, the purpose is to present the principle.

An attribute of neural networks that is important for the application in flight control is their capability for universal approximation of smooth functions. Hornik, Stinchcombe und White [4] produced evidence, that any nonlinear and smooth function can be approximated to an arbitrary accuracy using feedforward neural networks with just one hidden layer, given a sufficient number of hidden nodes.

### 2.4.1. A-Priori Knowledge

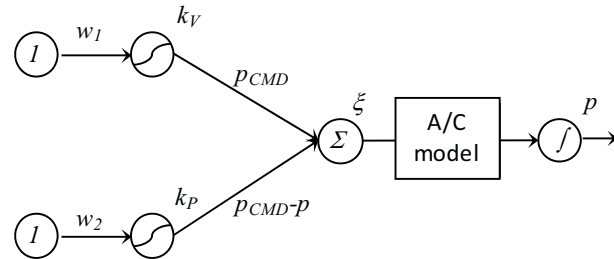
If there is some knowledge available about a system, that has to be identified or optimized, the optimization phase can be accelerated and the results improved, if this a-priori-knowledge is used for the design of the system model. For neural networks with a modular structure, the value range and start values of a module output can be adjusted by an offset and a scaling factor. For example, the controller gains were assigned to a value range from -10.5 to -0.5, to avoid positive numbers.

It was decided to implement one forward branch and one feedback loop. Therefore one module for each part was realized by one nonlinear activation function.

### 2.4.2. Structure

The controller structure comprises adaptive elements (gains), smooth bounded candidate functions and two branches (feedforward and feedback loop).

To allow the interpretation as weights, constant values of one serve as inputs. The outputs of the two basis functions represent the gains  $k_v$  and  $k_p$ . In contrast to the weights of layer one ( $w_1, w_2$ ), which are adjusted during the training phase, the input weights in layer two are not trainable. The values of  $p_{CMD}$  and of  $p_{CMD-p}$  for these connections are taken from the input data. The output sums both contributions to control surface deflection, calculated in the feed-forward control branch and in the feedback branch.



Legend:

- Smooth bounded candidate function (hyperbolic tangent)
- Summand
- Integrator
- Constant input of 1

FIGURE 3: Simple network structure used for adaptive control

Mathematics is quite simple for a network with a structure given in FIGURE 3. To calculate the results from a given input (here:  $p$  and  $p_{CMD}$ ) the following equations have to be solved:

$$(2) \quad k_v = \tanh(1 \cdot w_1) \cdot y_{factor1} + y_{offset1}$$

$$(3) \quad k_p = \tanh(1 \cdot w_2) \cdot y_{factor2} + y_{offset2}$$

$$(4) \quad \xi = k_v \cdot p_{CMD} + k_p \cdot (p_{CMD} - p)$$

The hyperbolic tangent function is a popular activation function and was selected for the nonlinear representation. If there is some a-priori knowledge available about the value range of the controller gains, then the output can be adjusted by a scaling factor ( $y_{factor}$ ) and an offset ( $y_{offset}$ ).

The first approach here was to reduce the complexity of the system as far as possible. If there is a need to model nonlinearity at a higher order, more complex approximator structures may be used. If any a-priori structure of the nonlinearity is known, it makes sense to utilize this knowledge in the structural layout of the combination of basis functions.

In some cases, a nonlinear dependency from input parameters is modeled within Flight Control Systems. For example, the Mach number has effect on the flight

dynamics and therefore the nonlinear characteristic in the transonic regime has to be modeled accurately. The structure could be modified appropriately by exchanging the constant input to a variable input driven by the mach number.

### 2.4.3. Smooth bounded candidate functions

Using smooth bounded candidate functions for the representation of adaptive controller gains helps to damp oscillations during the training phase due to variable adaptation increments  $\Delta w_{ij}$ . These increments to the weights are directly proportional to the gradient of the candidate function  $f'$  (see equation (13, 14) and FIGURE 5).

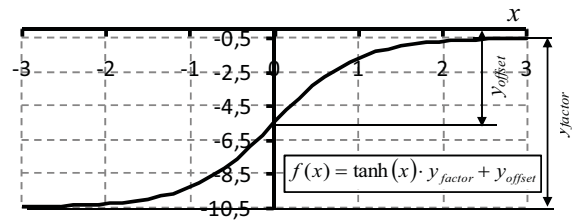


FIGURE 4: Hyperbolic tangent as activation function with customized boundaries

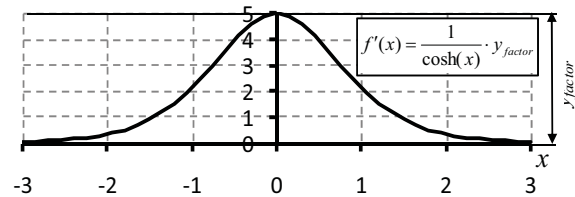


FIGURE 5: First derivative of the activation function

Furthermore, analytical bounds are known for the adaptive parameters.

## 2.5. Adaptation Law

### 2.5.1. Backpropagation

Backpropagation is a popular method for networks weight update, especially if the network structure is composed by multiple layers. It is used to modify the network weights based on an error, which was measured at the output. The magnitude of weight-changes is dependent from the error surface gradient, which is calculated for each neuron.

The Backpropagation algorithm can be used in an online or an offline mode. The difference between both modes is the amount of training data. Here an online mechanism is applied, where only the current state of the aircraft is used for training and no previous data is stored.

A network structure may be interpreted as multiple nested functions. Backpropagation is nothing else than differentiating the structure against the normal signal flow using the chain rule.

The labeling of a multilayer network structure is shown in FIGURE 6.

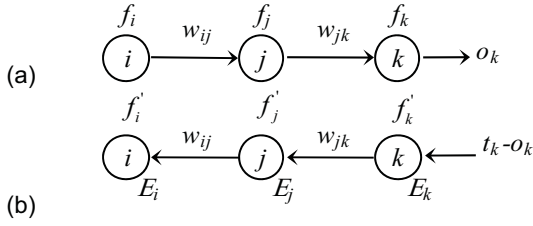


FIGURE 6: Labeling the forward output calculation (a) and backward error calculation (b)

The standard Back-Propagation Algorithm [7] calculates the output of the network  $o_k$  layer by layer from the first layer (left side) to the last layer (see FIGURE 6(a)). The network error  $E_k$  is calculated at the output. Beginning at the last layer, this network error is propagated through all preceding layers (see FIGURE 6(b)) until the first layer by the following equations:

Case: output layer

$$(5) \quad E_k = f'_k \cdot (t_k - o_k)$$

Case: hidden layer

$$(6) \quad E_j = f'_j \cdot w_{jk} \cdot E_k$$

$$(7) \quad E_i = f'_i \cdot w_{ij} \cdot E_j$$

With reference to FIGURE 3 and to be analogous to equations (5-7) the overall output error  $E_p$  and the hidden error  $E_\xi$  are defined as:

$$(8) \quad E_p = p_{PT1} - p$$

$$(9) \quad E_\xi = f'_\xi \cdot w_{\xi p} \cdot E_p$$

$$(10) \quad E_v = f'_v \cdot p_{CMD} \cdot E_\xi$$

$$(11) \quad E_p = f'_p \cdot (p_{CMD} - p) \cdot E_\xi$$

Based on these error calculations, the learning rules can be defined as follows.

$$(12) \quad \Delta w_{ij} = \eta \cdot o_i \cdot E_j$$

Equation (12) refers to FIGURE 6 and is valid in general for all layers. With reference to equations (9-11) the weight modifications of the first layer of the adaptive controller are calculated as follows:

$$(13) \quad \Delta w_1 = \eta \cdot 1 \cdot E_v = \eta \cdot f'_v \cdot p_{CMD} \cdot E_\xi$$

$$(14) \quad \Delta w_2 = \eta \cdot 1 \cdot E_p = \eta \cdot f'_p \cdot (p_{CMD} - p) \cdot E_\xi$$

## 2.5.2. Error Signal

As there is no target value available for the desired control surface deflection, the Network error cannot be calculated directly. However, the deviation  $\delta$  from the state variable  $p$  to the commanded value  $p_{CMD}$  or better the desired response  $p_{PT1}$  can be observed (FIGURE 2).

For the calculation of the overall output error  $E_p$  all parameter are derived from simulation data. Unfortunately this is not the case for the hidden error  $E_\xi$ , but this network error can be derived as follows.

The first derivative of the angular momentum for the rolling motion is defined as:

$$(15) \quad \frac{\partial B}{\partial t} = I_x \cdot \dot{p} = L$$

Here, the calculation of the rolling moment  $L$  is simplified and reduced to the major aerodynamic derivatives  $c_{l\xi}$  and  $c_{lp}$ :

$$(16) \quad L = \frac{\rho}{2} v^2 \cdot A \cdot s \cdot \left( c_{l\xi} \cdot \xi + c_{lp} \cdot p \frac{s}{2v} \right)$$

The equation of motion for the roll axis is defined as:

$$(17) \quad \dot{p} = \frac{\rho}{2} v^2 \cdot A \cdot s \cdot \left( c_{l\xi} \cdot \xi + c_{lp} \cdot p \frac{s}{2v} \right) \cdot \frac{1}{I_x}$$

To calculate the network error  $E_\xi$  according to equation (9), the network weight  $w_{\xi p}$  is needed. It can be calculated as follows:

$$(18) \quad w_{\xi p} = \frac{\partial \dot{p}}{\partial \xi} = c_{l\xi} \cdot \left( \frac{\rho}{2} v^2 \cdot A \cdot s \cdot \frac{1}{I_x} \right)$$

The second term in brackets of equation (18) is strictly positive. This fact is important for the convergence of the adaptation algorithm.

As we used a linear activation function for the output, its first derivative equals 1. Now the equation (9) can be formulated as follows:

$$(19) \quad E_\xi = c_{l\xi} \cdot \left( \frac{\rho}{2} v^2 \cdot A \cdot s \cdot \frac{1}{I_x} \right) \cdot (p_{PT1} - p)$$

Now we have an error signal that can be used for the Backpropagation algorithm to modify the weights accordingly.

**Note:** The error definition is based on the deviation between the output of the flight simulation  $p$  and the target function  $p_{PT1}$  and not between  $p$  and the commanded roll-rate  $p_{CMD}$ .

## 2.5.3. Adaptation performance

The adaptation speed and quality of the controller gains is closely connected to the learning-rate. A quick modification of the controller gains as response to a disturbance requires a high learning-rate ( $\eta = 0.5$ ). For a system operating under normal conditions, a low learning-rate is wanted to keep the controller gain modifications small ( $\eta = 0.1$ ).

Minor changes of the controller gains during agile maneuvers indicate, that the parameter setting is in the right order.

### 3. SIMULATION

#### 3.1. Simulation Environment

##### 3.1.1. Aircraft Simulation

The aircraft simulation model is based on a combat type aircraft with a total weight of 18 tons. It has a relaxed static stability and its longitudinal motion is controlled by a simplified flight control system model. The lateral motion is controlled by an asymmetric deflection of the ailerons and one rudder. The adaptive controller is embedded into the flight control system model and has only authority for the asymmetric deflection of the ailerons.

The nonlinear equations of motion are numerically integrated at 80Hz. Forces and moments are calculated from the aerodynamic model, mass & balance model and engine model. A simple actuator model is used, neglecting dynamic characteristics.

The aircraft simulation can be initialized, stopped and re-started by a user interface. A trim routine can be used to achieve a static wings-level attitude. The flight data was recorded for post processing purposes. The analysis was done in the time domain and the time histories were plotted for the relevant maneuver and parameter.

##### 3.1.2. Controller Simulation

The Controller Simulation environment was developed under C++ and provides some unique features such as a training algorithm for target slopes. Furthermore input-weights can be used additionally to conventional inputs. All object files were collected in a dynamic link library and were linked to the aircraft simulation.

The object-oriented programming of the Controller Simulation comprises the classes *Group*, *Layer*, *Node*, *Link*. Recurrent structures are possible, if one group is part of another super-group. Problem-oriented design of the network structure is possible. The I/O data of each group is accessible and can be monitored during operation.

##### 3.1.3. Controller Model Integration

The controller model is embedded into the aircraft simulation framework and synchronized to the simulation clock. After calculation of the aircraft model state parameters, the controller model computes the control surface deflection. This data is needed to calculate the aerodynamic forces within the aircraft simulation model. The response of the aircraft model is needed to calculate the network error as described in chapter 2.5.2. Now the weights are modified according to the learning-rules (13, 14). If the training mode is switched off, only the output of the controller network is calculated.

The controller model can be stored with the current values of the controller gains and can be reloaded for repeatability.

#### 3.2. Test procedure

The simulation was initialized always at the same condition, before a training or test maneuver was started. The initial flight attitude was a wings level flight trimmed at 230 knots (CAS) at an altitude of 9000 ft under standard atmosphere conditions (ISA). After two seconds of straight level flight a doublet maneuver with a commanded roll-rate  $p_{CMD}$  of  $\pm 20$  deg/s was initiated by a commanded step input to the roll controller. The roll doublet maneuver ended after a duration of twelve seconds. Another four seconds allow the aircraft to stop rolling. Afterwards a ramp maneuver with increasing roll-rate command up to 40 deg/s was initiated with a duration of four seconds. After a total time of 24 seconds the simulation was stopped.

#### 3.3. Case Studies

The purpose of the following case studies which are presented in this chapter is to demonstrate the capability of the aforementioned adaptive flight control within a simulation environment. Three different cases will be investigated, starting with the verification of the training results. The second case study will show the aircraft response, if its roll damping is reduced by 50%. This could be the case, if the aerodynamic model was inaccurate, or an unexpected configuration change occurred (e.g. structural defect). The third test case investigates the worst case scenario, if the controller gains are at their value limits, decreasing the stability of the overall system. For this case, the roll damping was not reduced.

The range of values for the flexible gains was always limited to  $]-10.5; -0.5[$  for all maneuvers.

##### 3.3.1. Case study #1, Training Quality

The intention of the first case study is to demonstrate, how well the adaptation law works. The criteria for an evaluation of this case study are:

- How long and how many maneuvers did the training algorithm take to find a static gain setting for stable flight?
- What is the quality of the simulation results operated without online adaptation in terms of damping, overshoot and target achievement?

After a training phase of hundred maneuvers, the controller gains read as follows:

$$\begin{aligned}k_v &= -6.71 \\k_p &= -6.07\end{aligned}$$

The time histories presented in FIGURE 7 show the results of a case study after training and without online adaptation. The values of the controller gains were fixed to the values mentioned above.



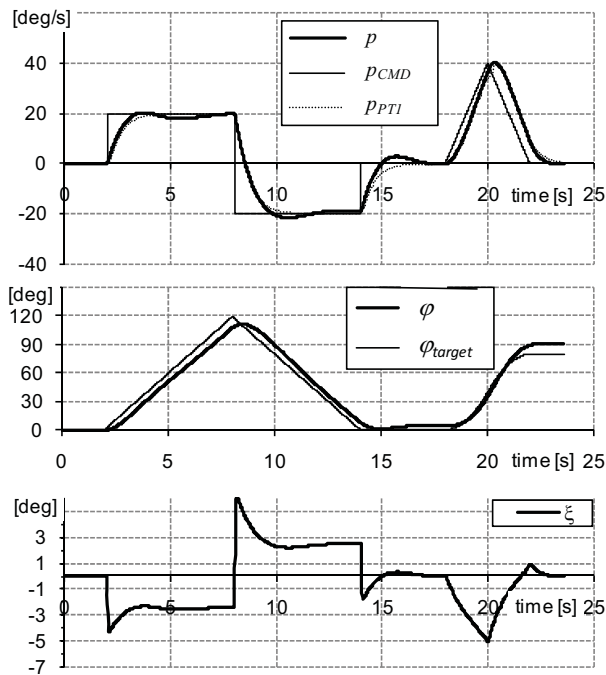


FIGURE 7: Test of training result (fixed gains)

After two seconds of level flight, the commanded roll-rate jumps to  $20 \text{ deg/sec}$  leading to a control surface deflection of  $-4.4 \text{ deg}$ . The commanded roll-rate is reached after further 1.5 seconds followed by a small overshoot.

For the commanded roll-rate of  $-20 \text{ deg/sec}$  a control surface deflection of  $6.5 \text{ deg}$  is calculated by the controller. The commanded roll-rate is reached after further 1.8 seconds followed by a well damped overshoot.

The ramp maneuver shows acceptable results in terms of target tracking and damping. This maneuver will be used as reference for the following case studies.

### 3.3.2. Roll-Damping Degradation

The following two case studies are a test for uncertainties in the aerodynamic model, which could lead to unacceptable handling qualities. The magnitude of the aerodynamic derivative for roll damping  $C_{lp}$  was reduced by 50%. The controller gains were taken from the reference. The first simulation was done without controller adaptation and the second simulation with activated adaptation.

#### 3.3.2.1. Case study #2, without Adaptation

This case study demonstrates the roll dynamic of an aircraft, whose roll damping was reduced by 50%, but the controller was not adjusted appropriate. The controller gains were initialized as they were identified with the aircraft having 100% roll damping:

$$\begin{aligned} k_v &= -6.71 \\ k_p &= -6.07 \end{aligned}$$

The two maneuvers (roll doublet and ramp) were performed without adaptation. Compared to the reference (FIGURE 7) one can see that the damping is lower,

leading to large overshoots in roll-rate and bank angle (about 40 deg).

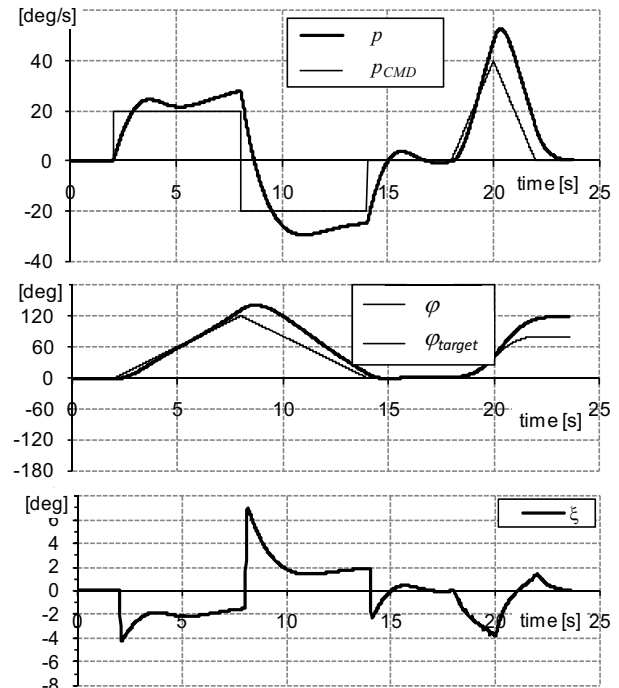


FIGURE 8: Aircraft with reduced roll damping (fixed gains)

The aircraft does not follow the commanded roll-rate in an acceptable way. The next case study will demonstrate, if the aircraft response could be improved with the help of an activated adaptation method.

#### 3.3.2.2. Case study #3, with Adaptation

This case study demonstrates the roll dynamic of an aircraft, whose roll damping was reduced by 50%. The controller gains were initialized as before. Now, the two maneuvers (roll doublet and ramp) were performed with an activated adaptation mechanism (FIGURE 9).

From the beginning of the roll doublet maneuver, the magnitude of the controller gain  $k_v$  is reduced. At the same time the magnitude of the controller gain  $k_p$  is increased.

After fifteen seconds of flight, no major adaptation is done, although there is a large network error ( $E\xi = 0.014$ ). This is a result of the adaptation law. If the commanded roll-rate is zero, no changes to the feed-forward branch are made (equation 13). On the other hand, the feed-back branch is adapted only a little, because the controller gain  $k_p$  is close to the boundary leading to small weight changes according to (14) and the slope of the candidate function (see FIGURE 5). But, the proportional dependency between the gain changes and the magnitude of the network error is obvious.

For this case study, the learning rate was set to  $\eta = 0.5$ . Both maneuvers show an acceptable response, in particular the ramp maneuver.

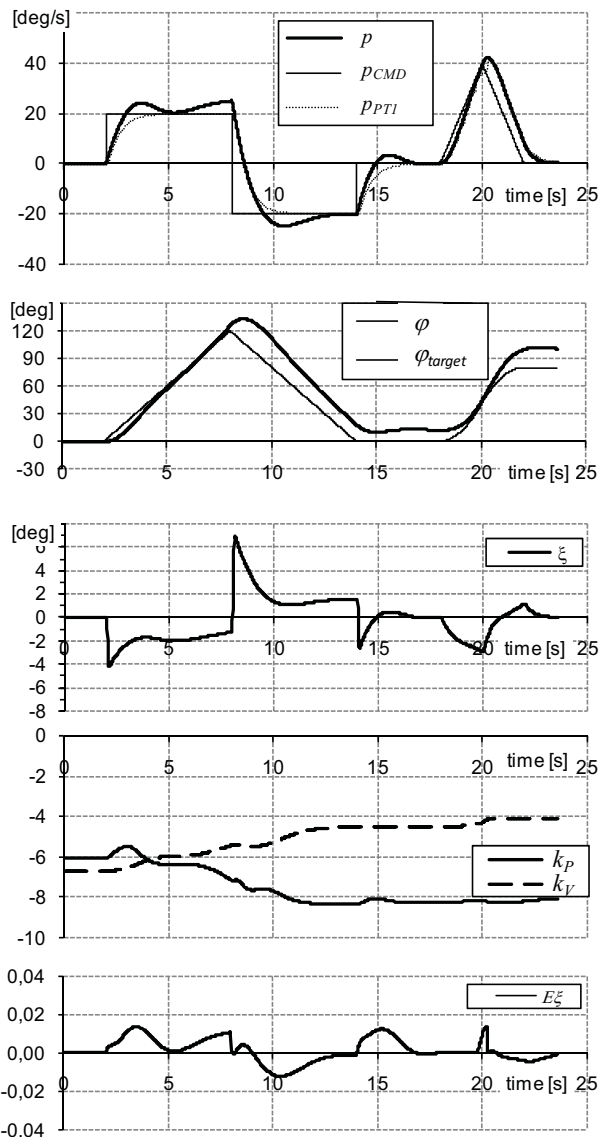


FIGURE 9: Aircraft with reduced roll damping (flexible gains)

These case studies demonstrate the influence of an adaptation mechanism to the aircraft response, in case of a roll-damping degradation. However this study does not reflect the worst case scenario.

### 3.3.3. Case Study #4, Worst Case and Recovery

The Worst Case reflects the situation, when both controller gains have values leading to insufficient stability of the overall system. This can be expected for values near the boundaries of the candidate functions value facet. As explained in chapter 2.5, the gradient descend method adapts very slowly, when the activation function converges against their limits. This test is a synthetic case, which is unlikely to arise during operation, but should not be excluded in this study.

It has to be mentioned again, that for this case study no degradation in roll-damping was defined.

For this worst case the initial values for the controller gains were selected as follows:

$$k_v = -10.0$$

$$k_p = -0.7$$

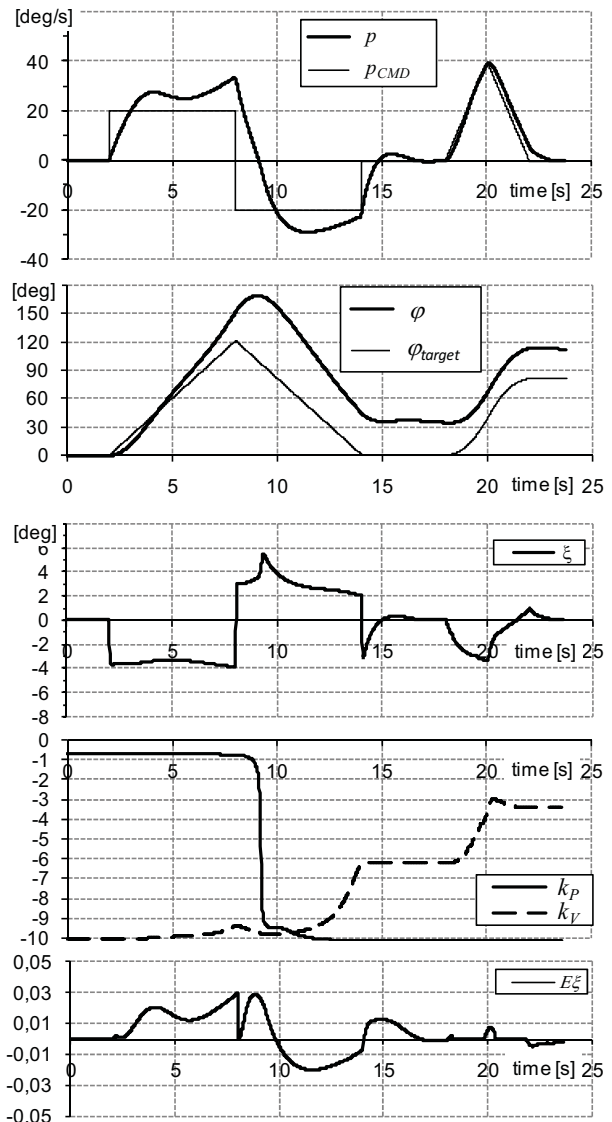


FIGURE 10: Worst case maneuver and recovery with online training (flex gains)

The initial setting of the gains leads to overshoots in the roll doublet maneuver, due to lack of feedback loop and strong forward command. After about eight seconds of flight, the network error  $E_{\xi}$  reaches its maximum. Consequently the controller gain  $k_p$  is adapted very quick under this condition, leading to a significant increment to the control surface deflection  $\xi$ . Further changes to  $k_v$  are made even during the second maneuver, while the network error  $E_{\xi}$  is moderate.

With the modified gain setting, the second maneuver (ramp) matches the target slope of the commanded roll-rate much better, compared to the first maneuver.

This maneuver was initiated with a worst case setting of the controller gains. One can expect, that the target values equal the values that were the result after the training

phase. It has to be pointed out, that during one maneuver a new gain setting was found by the adaptation algorithm that provides an acceptable aircraft response.

$$\begin{aligned}k_v &= -3.4 \\k_p &= -10.2\end{aligned}$$

But it is obvious, that this new gain setting reflects not the optimum setting, which was found after training.

#### 4. DISCUSSION

Some case studies were performed here, demonstrating the stability of the controlled aircraft system, if the adaptation mechanism is activated. So far, the adaptation law in combination with smooth bounded candidate functions provides stability for the controlled system from empirical assessment. The evaluation criteria, which were used for assessment of the case studies are summarized here:

- Duration until the control parameter reaches the commanded value the first time.
- Damping, overshoot magnitude
- Static deviation
- Adaptation characteristics

The controller network was structured, assuming that the gains have to be independent from any input data and are fixed as far as the adaptation mechanism is deactivated. For this the controller is regarded as linear. With an activated adaptation mechanism, the controller gains get dependent from the network error  $E_{\xi}^{\epsilon}$ . For this case, the controller is regarded as nonlinear. The dependency of the roll authority from state variables such as angle of attack, angle of sideslip and mach number is implicitly modeled, as a deviation between commanded value and actual state (=network error) results always in a adaptation of the controller gains. This implicitly accounts for off-axis dynamics.

A prospective application in aeronautics could be a flight control of small or micro UAVs. Especially in this sector unconventional designs for airplane and flight control system came up in the past and reveal new approaches for low-cost system development.

The Neural Network based approach, which was used for this Adaptive Flight Control, brings along two evaluation criteria, which are shown in TABLE 1. The correlation factor  $r$  describes the coherence between the actual roll-rate and the target roll-rate. The Mean Squared Error (MSE) describes the matching between the actual roll-rate and the target roll-rate. Both evaluation criteria demonstrate, that case study #1 and #3 show better results than case studies #2 and #4.

Case Study	Correlation coefficient $r$ $r = \frac{\text{Cov}(p_{PT1}, p)}{\sigma_{p_{PT1}} \cdot \sigma_p}$	MSE $\frac{1}{n} \cdot \sum_{i=1}^n \frac{1}{2} (p_{PT1,i} - p_i)^2$
#1, REF.	0,995	0,24
#2, NoAdapt.	0,988	2,28
#3, WithAdapt.	0,992	1,28
#4, Recover	0,973	15,28

TABLE 1. Evaluation parameters showing response quality

#### 5. CONCLUSIONS

The case studies presented here, demonstrate a proof of concept based on the idea, that an adaptive flight control using smooth bounded candidate functions could be applied to applications in aeronautics. The results show that the adaptive controller provides stability for the simulated aircraft, even in the case of faulty aerodynamic modeling. If the controller structure and the parameter setting is defined properly to the aircraft configuration, no further adaptation of the gains is needed during operation to provide acceptable controller characteristics. The authors are well aware of the numerous other efforts in the field of adaptive flight control and their high level of maturity. Furthermore the necessity for a stability proof and traceable and deterministic V&V strategies is clear. The publication just presents the proof of concept encouraging to further assessment of the smooth activation functions and the active incorporation of a priori knowledge in designing the networks.

The case studies demonstrated a well damped control characteristic and a fast adaptation behavior. In the case of a roll-damping degradation, the controller gains were adapted within one roll doublet maneuver, demonstrating a well damped roll maneuver characteristic. The method and the results provide a valuable contribution for adaptive flight control for future applications in aeronautics. The controller structure and the adaptation law were kept as simple as possible. Of course, the compliance with the certification requirements of adaptive flight control systems of UAS has to be demonstrated in the future.

With the help of the simulation environment, further research is done to investigate the system behavior under circumstances such as noisy signals or with other maneuvers. Currently a simple adaptive controller model is going to be implemented in a low cost flight control system embedded in a radio controlled flight model, in order to proof the concept in real flight.



## SYMBOLS AND ABBREVIATIONS

$A$	wing reference area
$B$	angular momentum
$c_{l\xi}$	aerodynamic derivative (aileron effectiveness)
$c_{lp}$	aerodynamic derivative (roll damping)
$D$	damping
$E$	error
$f$	candidate function
$I_x$	moment of inertia for the x-axis
$k_p$	controller gain for feedback loop
$k_v$	controller gain for roll steering
$n$	number of patterns
$o_k$	network output
$L$	rolling moment
$p$	roll-rate
$\dot{p}$	roll-acceleration
$p_{CMD}$	commanded roll-rate
$p_{PTI}$	optimal transfer function for a change in $p$
$\dot{p}_{PTI}$	first derivative of $p_{PTI}$
$r$	correlation coefficient
$s$	wing span
$t_k$	teaching parameter for neural network
$v$	true air speed
$w_{1,2}$	weights for trainable network connections
$\Delta w_{1,2}$	weight changes during training phase
$\delta$	error signal
$\beta$	sideslip angle
$\eta$	learning-rate
$\rho$	air density
$\sigma$	standard deviation
$\phi$	bank angle
$\xi$	aileron deflection

CAS	Calibrated Airspeed
I/O	Input/Output
ISA	ICAO Standard Atmosphere
MLP	Multi Layer Perceptron
MNN	Modular Neural Network
MRAC	Model-Reference Adaptive Control
MSE	Mean Squared Error
UAS	Unmanned Air System

## REFERENCES

- [1] HOLZAPFEL, F.: *Nichtlineare adaptive Regelung eines unbemannten Fluggerätes*, Dissertation, Technische Universität München, ISBN 3-89963-112-9, 2004
- [2] SEIFERT, J., WAGNER, O., ONKEN, R.: *Identifizierung nichtlinearer Derivative mit einem Modularen Neuronalen Netzwerk*, DGLR Deutscher Luft- und Raumfahrtkongress 2002, DGLR-2002-202, Stuttgart, 2002
- [3] SEIFERT, J.: *Identifizierung nichtlinearer aerodynamischer Derivative mit einem Modularen Neuronalen Netzwerk*, Dissertation, Universität der Bundeswehr, 2003
- [4] HORNIK, K., STINCHCOMBE, M., WHITE, H.: *Multilayer Feedforward Networks are Universal Approximators*. Neural Networks, Vol. 2, S. 359 – 366, Pergamon Press plc, 1989.
- [5] SLOTINE, J.-J.E.; LI, W.: *Applied Nonlinear Control*, Prentice Hall, New Jersey, ISBN 0-13-040890-5, 1991
- [6] BRINKER, J. S. and WISE, K. A.: *Flight Testing of a Reconfigurable Flight Control Law on the X-36 Tailless Fighter Aircraft*. AIAA-2000-3941. AIAA Guidance, Navigation, and Control Conference and Exhibit, Denver, CO, 14.-17. August 2000.
- [7] ZELL, A.: *Simulation Neuronaler Netze*, ISBN 3-89319-554-8, Addison-Wesley, Bonn, 1994